

Dipolar filtered magic-sandwich-echoes as a tool for probing molecular motions using time domain NMRJefferson G. Filgueiras,¹ Uilson B. da Silva,¹ Giovanni Paro,¹ Marcel N. d'Eurydice,² Márcio F. Cobo,¹ and Eduardo R. deAzevedo¹¹*Instituto de Física de São Carlos, Universidade de São Paulo, P.O. Box 369, São Carlos, 13560-970 SP, Brazil*²*School of Chemical and Physical Sciences, Victoria University of Wellington, PO Box 600, Wellington, New Zealand*

We present a simple ^1H NMR approach for characterizing intermediate to fast regime molecular motions using ^1H time-domain NMR at low magnetic field. The method is based on a Goldmann Shen dipolar filter (DF) followed by a Mixed Magic Sandwich Echo (MSE). The dipolar filter suppresses the signals arising from molecular segments presenting sub kHz mobility, so only signals from mobile segments are detected. Thus, the temperature dependence of the signal intensities directly evidences the onset of molecular motions with rates higher than kHz. The DF-MSE signal intensity is described by an analytical function based on the Anderson Weiss theory, from where parameters related to the molecular motion (e.g. correlation times and activation energy) can be estimated when performing experiments as function of the temperature. Furthermore, we propose the use of the Tikhonov regularization for estimating the width of the distribution of correlation times.

I. INTRODUCTION

The development of advanced materials with desired properties and function requires a thorough knowledge of the structural and dynamical properties of the molecular systems that comprise them. Many properties of synthetic and natural organic materials are closely related to the mobility of their molecules, making molecular motions a key point for understanding these systems¹⁻⁸. In this respect, Nuclear Magnetic Resonance (NMR) provides a variety of methods to access motion information in a wide frequency range (Hz-MHz)⁹⁻¹².

For solid systems, the NMR methods developed for probing molecular motions usually rely on the orientation dependence of the NMR frequencies, which provides high sensitivity to the time scale and geometry of segmental motions^{9,11,12}. Such features can be studied with unpaired precision by using samples with isotopic labeling, for instance ^2H and ^{13}C , at specific molecular segments. This approach, however, becomes uneconomical in studies of large molecules. When isotopic labeling is not possible (or desired), several high resolution solid-state NMR methods have been developed^{9,11-13}, giving site-resolved information about the molecular dynamics. However, they lack sensitivity due to the detection of low abundant nuclei, as ^{13}C , resulting in time consuming experiments. In contrast, ^1H based solid-state NMR methods provide high sensitivity, but loses in specificity, since the local character of the dipolar interaction is lost due to spin-diffusion¹⁴⁻¹⁹. Despite not being able to deliver details on the local geometry, ^1H solid-state NMR is useful to study the overall dynamical behavior and its temperature dependence, estimating the activation parameters of the motion.

Because of the high sensitivity of ^1H detection this experiments can be efficiently performed at low magnetic fields using much less expensive and simpler NMR spectrometers. Because of that, Time Domain ^1H NMR (TD-

NMR) at low magnetic field, became quite popular for studying soft matter, in particular polymer and biopolymer based systems²⁰⁻²³. There are many TDNMR techniques devoted to study molecular motions exploring either the relaxation phenomena¹⁶⁻¹⁸ or the motional averaging of the ^1H - ^1H dipolar interaction and its effect on the NMR signals²⁰⁻²³.

Here we address the effects of motions on common TD-NMR pulse sequences and propose an approach where a Goldmann-Shen type of dipolar filter²⁴, with duration t_f , is followed by a mixed Magic Sandwich Echo sequence (DF-MSE)²⁵. The dipolar filter suppresses the signal of ^1H in "rigid" segments (i.e. which the time-domain signal decays faster than the filter time), keeping the ^1H signal arising from more mobile segments. Thus, at low temperatures where all molecular segments are rigid, the signal will be completely suppressed and the intensity of the MSE echo will vanish. However, in a temperature where some molecular segments become mobile, the dipolar filter sequence no longer suppresses the signal and the MSE echo appears. Thus, the method will detect the onset temperature of specific molecular motions by the increase of the DF-MSE echo intensity as a function of temperature.

We also demonstrate that the filter time dependence of the normalized DF-MSE intensities acquired at a fixed temperature is sensitive to both the mean and the width of the distribution of correlation times. A simple formula based on the Anderson-Weiss approach²⁶ is then used as a kernel for Tikhonov regularization procedure providing a fit to the experimental data that allow to estimate the correlation time distribution in an independent fashion. Using this procedure we obtain the distributions of the correlation times and activation parameters of motions associate to the glass transition of amorphous polymers and compare our results with those obtained by other methods^{27,28}. All measurements were carried out in a time considerably shorter in comparison

to these other techniques.

The article is presented as follows. Section II is devoted to a short theoretical background, reviewing some key concepts. Section III discusses the results, presenting the method to detect the molecular motions along with some numerical simulations and experimental results on the characterization of the molecular motion in model amorphous polymers. At last, some discussions and conclusions are presented.

II. THEORY

A. Description of the DF-MSE pulse sequence

In this section we discuss an approach for the detection of molecular motions in the intermediate to fast frequency range (kHz-MHz) using a dipolar filter. In principle, any type of dipolar filter could be used^{29,30}, but we choose a slightly modified version of the simpler and well known Goldman-Shen (GS) dipolar filter²⁴. The most known application of GS filter is to suppress the signal of rigid segments in spin diffusion experiments, which aim to characterize domains sizes and interphases in heterogeneous polymers, like semicrystalline polymers, copolymers and polymer blends^{20,30,31}.

The basic GS pulse sequence consists of three pulses, see Fig. 1 ignoring the π pulses. The first pulse leads the magnetization to the xy -plane. During a waiting time t_f , called filter time, the magnetization due to rigid segments rapidly decays due to the strong ^1H - ^1H dipolar coupling. In contrast, the magnetization from mobile segments, i.e. which have the ^1H - ^1H dipolar coupling averaged by motions, remains after t_f and one of its component (x or y in consecutive scans) is stored in the z -direction in consecutive scans) is stored in the z -direction after the second pulse. The remaining component in the xy -plane after the second pulse is removed after t_z by proper phase cycling of the pulses. Thus, the magnetization after t_z is along the z -direction. Because the signal from strong dipolar coupled ^1H spins decay during t_f , the signal after the GS filter originates only in segments where the ^1H - ^1H dipolar coupling is reduced by molecular motions. Thus, t_f defines the upper limit for the motional rates that will be interpreted as rigid in the experiments.

When using the GS filter to probe molecular motion one should also consider segments that do not move fast enough to fully average the ^1H - ^1H dipolar couplings. In this case the evolution under residual ^1H - ^1H dipolar couplings during the GS sequence can generate multiple quantum coherences (MQCs) during t_z . These MQCs can be converted into transverse magnetization by the third pulse, leading to artifacts in the detected signal³². In the present case, the single and double quantum coherence existing during t_z have their effects canceled by cycling the phases of the first two pulses, with respect to the third, in steps of 90° ³³.

Another point to be considered concerns the static magnetic field inhomogeneity. For highly inhomogeneous

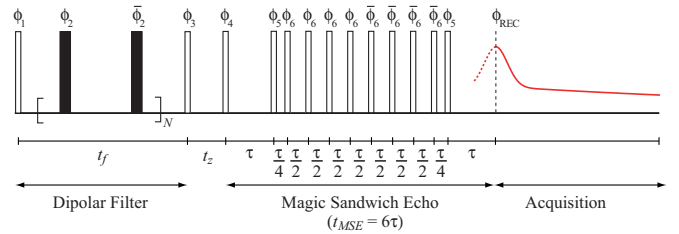


FIG. 1. The DFMSE pulse sequence, the signal after the GS dipolar filter comes solely from the slow-decaying components, the MSE pulse train is employed to overcome the experimental dead time. The filled rectangles indicate the π pulses, while all the other pulses are $\pi/2$ rotations. The phase cycling is given in Table I.

TABLE I. Phase cycling for the DFMSE pulse sequence.

Step	ϕ_1	ϕ_2	ϕ_3	ϕ_4	ϕ_5	ϕ_6	ϕ_{REC}
1	0	90	180	0	270	0	180
2	0	270	0	0	90	0	180
3	90	0	270	0	90	0	180
4	90	180	90	0	270	0	180
5	180	90	0	0	0	270	0
6	180	270	180	0	180	270	0
7	270	0	90	0	180	270	0
8	270	180	270	0	0	270	0

magnetic fields, as typical in TDNMR, the decay of the signal during t_f is dictated by the magnetic field inhomogeneity. As a result, the upper limit for t_f would be defined by the field inhomogeneity. To overcome it we added a train of π pulses³⁴ during t_f , see Fig. 1. We remark that such π pulses have no effect on the spins evolution under the ^1H - ^1H dipolar coupling if the pulse lengths are much shorter than the inverse of the dipolar coupling strength.

The signal from strong dipolar coupled ^1H spins decays in few microseconds, so it is necessary to avoid significant loss of magnetization due to finite receiver dead time. This is achieved using a mixed-MSE of duration t_{MSE} before detection²⁵. The mixed-MSE sequence, displayed in the Fig.1, provides the refocusing of both the ^1H - ^1H dipolar coupling and the field inhomogeneities.

The intensity of the echo after applying the GS filter followed by the mixed-MSE pulse sequence is then

$$I_{DF}(t_f, t_{MSE}) = G(t_f)I_{MSE}(t_{MSE}), \quad (1)$$

where $G(t_f)$ and $I_{MSE}(t_{MSE})$ are, respectively, the functions defining the modulation in the original magnetization introduced by the application of the GS filter and the mixed-MSE sequence.

B. Detecting onset temperatures of molecular motions using the DF-MSE pulse sequence

The qualitative behavior of $I_{DF}(t_f, t_{MSE})$ offers information about the onset temperature of molecular motions in a very simple way, which can be quite useful for many multiphase systems, where the macroscopic properties are associated to molecular dynamics in different segments. Therefore, it is important to investigate the onset temperatures of dynamic processes in distinct segments or phases. In principle, this can be achieved using such as Differential Scanning Calorimetry (DSC), Dynamical Mechanical Thermal Analysis (DMTA) or Dielectric Relaxation^{35,36}. However, multiphase systems have wide distribution of motions and complexes structures. Consequently, DSC usually fails in detecting local motions or even bulk processes in highly heterogeneous systems. Although DMTA and Dielectric relaxation are both suitable methodologies, they may require special sample preparation, which is not always possible or easy. On the other hand, ^1H NMR based methods have good sensitivity, but the clear identification of the onset temperatures usually requires some data processing and simulations^{9,16}. Therefore, our aim here is to provide a direct and very straightforward way to identify the onset temperature of molecular motions in TDNMR using the DF-MSE experiment.

Our approach resembles previous works by Saalwächter and co-workers which used the measurement of the intensity of a mixed-MSE echo $I_{MSE}(t_{MSE})$ as a function of temperature. In principle, for rigid systems the temperature dependence of $I_{MSE}(t_{MSE})$ is dictated by the Curie law, i.e., proportional to T^{-1} . However, molecular motions occurring with rates in the order of the inverse of the ^1H - ^1H dipolar coupling interfere with the echo formation, reducing the signal intensity in a Curie law independent fashion. Thus, by monitoring the echo intensity as a function of temperature, the onset of molecular motions can be probed as the deviation from the Curie law at temperatures where the motion sets on. In reference²² it was shown that the normalization of the echo intensities by the Curie temperature dependence provides a clear way of detecting the onset temperature of molecular motions, such as glass transition²² or local flips of polymer chains³⁷. It is worth mentioning that the signal intensity may vary as a function of temperature due to instrumental reasons, for example, the efficiency of the pulses and resonance offsets may change with temperature.

Here we use the same principle, but with the DF-MSE pulse sequence. In this case the temperature variations of the signal due to factor unrelated to motion can be minimized by the normalization of $I_{DF}(t_f, t_{MSE})$ by the intensity of a signal acquired with short t_f , so the GS dipolar filter have no effect. Supposing that the temperature variation of the signal by factors other than motion could be encoded in a parameter $\alpha(T)$, one can build the normalized intensity as

$$\begin{aligned} I_{DF}^N(t_f, T) &= \frac{G(t_f, T)I_{MSE}(t_{MSE}, T)\alpha(T)}{G(0, T)I_{MSE}(t_{MSE}, T)\alpha(T)} \\ &= \frac{G(t_f, T)}{G(0, T)}. \end{aligned} \quad (2)$$

Interestingly, the normalized intensity only depends on the effect of the GS dipolar filter on the signal intensity. The onset temperature of specific molecular motions will be detected by the increase of the DF-MSE echo intensity as a function of temperature, which will be seen as a change in the slope of the DF-MSE echo $I_{DF}^N(t_f, T)$ vs. T curve.

C. Quantifying motion effects using DF-MSE

Here we discuss the dependence of the signal I_{DF} as a function of the parameters related to the molecular motion. First, we show how the correlation time affects the intensity of the detected echo as well as the width of the distribution of correlation times. The description in terms of the temperature is carried out using an Arrhenius activation function, but can be easily extended to other activation functions such as Vogel-Fulcher-Tammann (VFT) or William-Landel Ferri (WLF)³⁸. So, we are able to check how parameters like the activation energy and the Arrhenius pre-factor affect the DF-MSE signal.

As stated in Eq. (2), the normalized intensity I_{DF}^N depends only on the motion effects encoded during the GS filter, i.e $G(t_f)$. This is a simple free induction decay (FID) during t_f , for which the motion effects can be well predicted in the framework of the Anderson and Weiss approach^{22,26}.

According to the Anderson-Weiss approximation of a stationary correlation function²⁶, the FID is described by

$$G(t) = \exp\left(-M_2 \int_0^t (t - \tau)K(\tau)d\tau\right), \quad (3)$$

where $K(\tau)$ is the memory function, i.e., the normalized correlation function of the shifted frequencies due to the local fields, and satisfies $K(0) = 1$. M_2 is the second moment of the distribution of local fields in the absence of molecular motions.

Considering homonuclear spin systems, the local field distribution is defined by the ^1H - ^1H dipolar coupling, which has a Gaussian profile³⁹⁻⁴¹. Also assuming isotropic rotational diffusion of the molecules⁴²⁻⁴⁴, the memory function is given by²⁶

$$K(\tau) = \exp\left(-\frac{|\tau|}{\tau_c}\right),$$

where τ_c is the correlation time of the motion. Within these approximations, the normalized FID signal is written as

$$G(t) = \exp\left(-M_2\tau_c^2(\exp(-t/\tau_c) + t/\tau_c - 1)\right). \quad (4)$$

A more detailed discussion of the formalism is presented in^{40,41,43}.

Therefore, the normalized intensity $I_{DF}^N = \frac{G(t_f, \tau_c)}{G(0, \tau_c)}$ becomes

$$I_{DF}^N(t_f, \tau_c) = \exp(-M_2 \tau_c^2 (\exp(-t_f/\tau_c) + t_f/\tau_c - 1)) \quad (5)$$

Note that the temperature dependence in Eq. (2) is related to τ_c by the activation function of the motion.

Fig. 2 (a) shows calculated I_{DF}^N as a function of τ_c , for different t_f and $M_2 = 6 \times 10^9$ (rad/s)². As the correlation time decreases the dipolar coupling starts to be averaged out by the molecular motions, leading to a remaining magnetization after the dipolar filter. The amplitude of this magnetization increases until the correlation time is short enough to fully average the ¹H-¹H dipolar coupling, so the filter has no effects on the magnetization during the filter time. We also observed that the range of correlation times that I_{DF}^N is sensitive to the motion, i.e. the dynamic window of the experiments, can be adjusted by setting the filter times t_f . It is worth mentioning that the dynamical window is limited by the relaxation times T_1 , as the signal starts to show relaxation effects during t_f rather than simple averaging of the ¹H-¹H dipolar coupling. Note that the effect of the random fluctuation of the dipolar fields, i.e. T_2 , is taken into account in the AW theory.

The previous equation is restricted to the case of motions occurring with a single correlation time. Since many systems have heterogeneous dynamics, one must consider the case where the motion occurs with a distribution of correlation times. This can be achieved by calculating the I_{DF}^N intensity as a sum of the intensities given by Eq. (5) weighted by the distribution of correlation times function $g(\tau_c)$, i.e.,

$$I_{DF}^N(t_f) = \int_0^\infty I_{DF}^N(t_f, \tau_c) g(\tau_c) d\tau_c, \quad (6)$$

To demonstrate the effects of the distribution of correlation times on I_{DF} we assume a log-gaussian distribution of correlation times^{45,46} which can be characterized by two parameters, the standard deviation of the distribution σ and the center of the distribution in the log scale $\langle \ln \tau_c \rangle$, see caption of Fig. 2. Fig. 2 (b) shows a set of curves calculated for I_{DF}^N as a function of $\langle \tau_c \rangle$ for different σ values. As it can be observed, the larger the value of σ , the wider the I_{DF}^N vs. $\langle \tau_c \rangle$ curves. This occurs because the amount of segments moving inside a fixed dynamical sensibility window, defined by t_f , changes more slowly with increasing $\langle \tau_c \rangle$ as σ .

D. Temperature dependence of DF-MSE signals

To check the signal dependence on the temperature, we discuss how each of the parameters in the activation

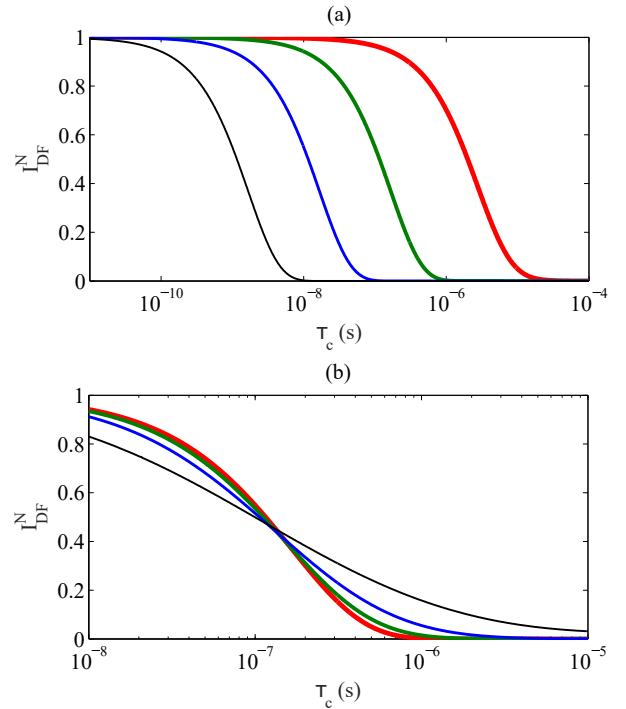


FIG. 2. I_{DF}^N as a function of correlation times. For different filter times, (i) shows the sensitivity of the dipolar filter. The simulations were carried out with a single correlation time, for $t_f = 50 \mu\text{s}$ (red, thickest), $1000 \mu\text{s}$ (green), $10000 \mu\text{s}$ (blue) and $100000 \mu\text{s}$ (black, thinnest). Below, we show the effects of a distribution of correlation times, assumed to be a log-gaussian distribution $g(\tau_c, \sigma, \langle \tau_c \rangle) = \exp(-\frac{(\ln \tau_c - \langle \ln \tau_c \rangle)^2}{2\sigma^2}) / \sigma\sqrt{2}$, where $\langle \tau_c \rangle$ is the average correlation time and σ is the standard deviation. For a fixed filter time $t_f = 1000 \mu\text{s}$, we made calculations for $\sigma = 0.1$ (red, thickest), 0.5 (green), 1.0 (blue) and 2.0 (black, thinnest).

function modify the signal. For the sake of simplicity, only the Arrhenius function is considered in the calculations, but similar behaviors are observed when using other activation functions³⁸. According to the Arrhenius activation function the mean correlation time can be converted into temperature using two activation parameters, the apparent activation energy E_a and the prefactor τ_0 , i.e.,

$$\ln \left(\frac{\langle \tau_c(T) \rangle}{\tau_0} \right) = \frac{E_a}{RT}, \quad (7)$$

R is the gas constant. Fig. 3 shows $I_{DF}^N(t_f, T)$ vs. T curves calculated with different values of the E_a and τ_0 . The calculations were carried out using a filter time of $50 \mu\text{s}$, which is long enough to suppress the contribution of the signal from rigid segments. In Fig. 3(a), the signal $I_{DF}^N(t_f, T)$ is calculated for different values of E_a . The curve is shifted to higher temperatures as E_a increases, with a small decrease on its slope. If τ_0 is changed, the dynamic window is also translated, with a more signifi-

cant decrease in the curve slope, as can be seen in Fig. 3(b).

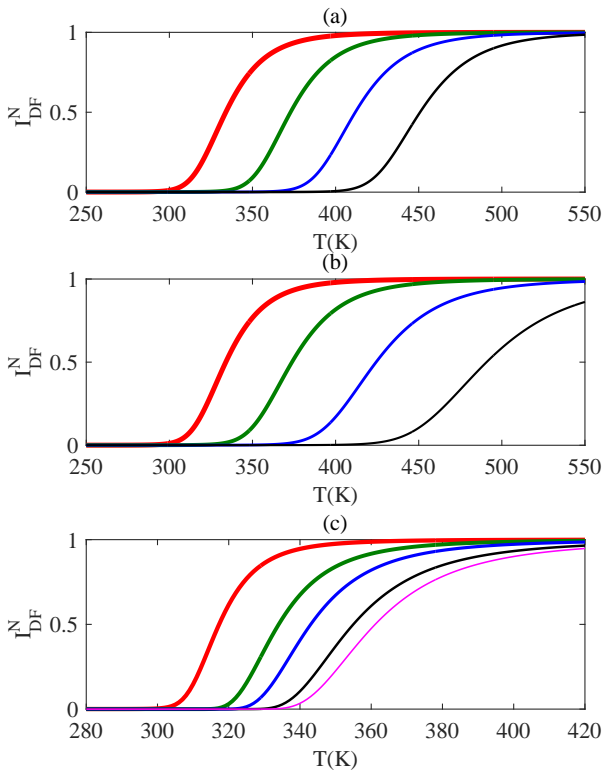


FIG. 3. Signal dependence on temperature. Each curve in (i) is simulated for a different value of the activation energy, while the Arrhenius prefactor is kept constant at $\tau_0 = 10^{-15}$ s. E_a takes the values 60 kJ/mol (red, thickest), 67 kJ/mol (green), 74 kJ/mol (blue) and 81 kJ/mol (black, thinnest). (ii) exhibits how the Arrhenius prefactor affects I_{DF}^N . $E_a = 60$ kJ/mol for all curves. τ_0 values are 10^{-15} s (red, thickest), 10^{-14} s (green), 10^{-12} s (blue) and 10^{-12} s (black, thinnest). For both (i) and (ii), the filter time is set to $50 \mu\text{s}$. Simulations for different filter times are shown in (iii), with $E_a = 60$ kJ/mol and $\tau_0 = 10^{-15}$ s. The filter times are $50 \mu\text{s}$ (red, thickest), $250 \mu\text{s}$ (green), $800 \mu\text{s}$ (blue), $2000 \mu\text{s}$ (back) and $3000 \mu\text{s}$ (magenta, thinnest).

E. DF-MSE difference curves

So far, we discussed how the Goldman-Shen dipolar filter is suited to probe molecular motions and to estimate the activation parameters of such motions. It is important to exploit ways to quantify the kinetic parameters itself, i.e., the correlation times and their distributions.

It is worth mentioning that the effects of a distribution of correlation times are hard to take into account, since a model for the distribution width as a function of the temperature is not known, to the best of our knowledge. Wachowicz *et al.* applied a linear model to describe $\sigma(T)^{27,47}$, however, this is not a generally expected behavior. Indeed, more elaborated and time consuming ^2H

and ^{13}C exchange NMR experiments have been used to extract the width assuming log-gaussian or Kohlrausch-Williams-Watts (KWW) correlation functions. Thus, a fast method capable to estimate the distribution of correlation times, without previous assumptions, is highly desirable.

Fig. 3 (c) shows the signal dependence on temperature for different filter times. As the filter time increases, the strenght of the dipolar filter is increased, which implies on the dynamical window moving to smaller correlation times, i.e., higher temperatures. Hence, the choice of the filter time sets the cut-off motion rate detectable by the dipolar filter. Based on this idea one can take the differences between two $I_{DF}^N(t_f, \tau_c)$ intensities with different filter times (t_f^{min} and t_f) to obtain a well defined dynamic window.

$$I_{diff}(t_f, t_f^{min}, \tau_c) = I_{DF}^N(t_f^{min}, \tau_c) - I_{DF}^N(t_f, \tau_c). \quad (8)$$

Considering the τ_c dependence, $I_{diff}(t_f, t_f^{min}, \tau_c)$ is null when the signals acquired with t_f^{min} and t_f are equal and nonzero whenever they are different. Therefore, the nonzero region of $I_{diff}(t_f, t_f^{min}, \tau_c)$ defines the τ_c boundary of a well defined dynamic window. If the motion occurs with a distribution of correlation times $I_{diff}(t_f, t_f^{min}, \tau_c)$ will depend on how many segments moves within the specified dynamic window, i.e. on the distribution of correlation times itself. To have the widest dynamic window possible, we choose the minimum filter time, t_f^{min} , as the shortest one without any signal from the rigid segments. It is worth mentioning that the quantity above keeps its dependence with the correlation times, just like $I_{DF}^N(t_f, \tau_c)$. Besides, establishing a well defined dynamical window enhances the dependence of the distribution of correlation times. Taking into account the motion heterogeneity of the system Eq. (8) becomes a sum over the correlation times weighted by the corresponding distribution $g(\tau_c)$, i.e.,

$$I_{diff}(t_f, t_f^{min}) = \int_0^\infty I_{diff}(t_f, t_f^{min}, \tau_c) g(\tau_c) d\tau_c. \quad (9)$$

F. Extracting the distribution of correlation times from the filter time dependence of I_{diff}

For fixed $\langle \tau_c \rangle$ and t_f^{min} the dependence of $I_{diff}(t_f, t_f^{min})$ on t_f encodes the distribution of correlation times. This quantity can be easily obtained experimentally by measuring a set of normalized DF-MSE echoes at fixed temperatures and with filter times ranging from t_f^{min} to t_f^{max} . Assuming a specific shape for the distribution of correlation time, like a log-gaussian distribution, $I_{diff}(t_f, t_f^{min})$ vs. t_f can be calculated for various $\langle \tau_c \rangle$ and σ . The fit of these calculated curves to the experimental data provides the values for $\langle \tau_c \rangle$ and σ .

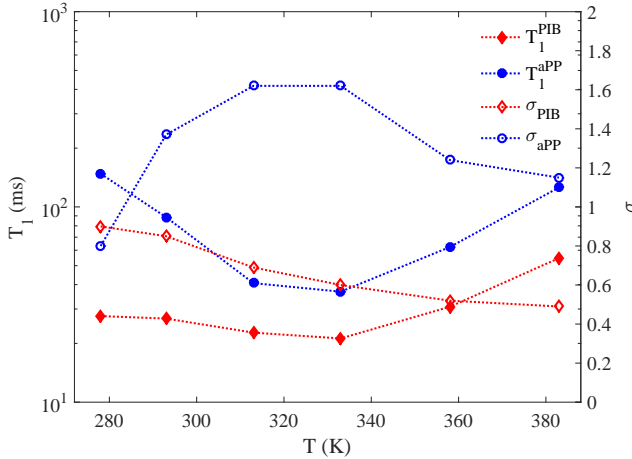


FIG. 4. Standard deviations of the distributions of correlation times and measured values of T_1 . The red diamonds depict the PIB data, while blue circles exhibit the aPP data. The filled symbols are the standard deviations.

A similar procedure has been used with different NMR methods^{23,27,46–49}.

However, Eq. (9) is a Fredholm integral of first kind, which means that if the exact expression of $I_{diff}(t_f, t_f^{min})$ is known it can be used as a fitting Kernel in a Tikhonov regularization procedure. Such procedure allows us to extract $g(\tau_c)$ without any previous assumption on the shape of the distribution. Interestingly, this can be done for several temperatures independently, so the temperature dependence of $g(\tau_c)$ can be obtained. Moreover, once $g(\tau_c)$ is known, it is straightforward to extract the $\langle \tau_c \rangle$, so the motion activation function can also be properly mapped. There are some drawbacks on this approach. First, the Anderson Weiss treatment considers isotropic rotation diffusion, so geometrically restricted motions are not covered. This can be relaxed choosing a proper AW formula adapted to restrict rotations. However, it requires some knowledge on the dynamic order parameter of such motions^{40,41,50}. Second, the ambiguities on the Tikhonov regularization, mainly considering the choice of the regularization parameter are well known⁵¹, so a good set of data, with enough t_f points and minor experimental noise and artefacts, is required. Since we are dealing with ^1H acquisition and the pulse sequence of Fig. 1 is quite robust to experimental artefacts, we believe such approach is suitable.

III. EXPERIMENTAL RESULTS

NMR: measurements were performed on a 20 MHz Bruker MINISPEC. The ^1H π and $\frac{\pi}{2}$ pulse lengths were $2.5\mu\text{s}$ and $5\mu\text{s}$, respectively. We measured T_1 using a standard inversion-recovery sequence, and we set the recycle delays to $5T_1$. The Magic Sandwich Echo (MSE) sequence was performed with echo times of $100\mu\text{s}$. Dipolar

filtered MSE experiments were carried out using a Goldman-Shen filter sequence varying the filter times t_f .

Samples: The samples used in the experimental demonstrations were atactic poly(propylene): aPP [$\text{CH}_2\text{-CH}(\text{CH}_3)\text{-}$], $M_w = 118000$ g/mol, $T_g = 251$ K and poly(isobutylene): PIB [$\text{CH}_2\text{-C}(\text{CH}_3)_2\text{-}$], $M_w = 2400000$ g/mol, $T_g = 205$ K. Both samples are fully amorphous. We measured the second moment for both samples fitting the FID, at 173 K, with the Abragam function⁵². The values obtained were $(6.62 \pm 0.09) \times 10^9$ (rad/s)² and $(8.96 \pm 0.03) \times 10^9$ (rad/s)², for the aPP and PIB, respectively. More details about the samples can be found in references^{28,49}. The temperature was controlled using a Bruker BVT3000, with a 2 K resolution on the sample.

A. Estimating correlation times distributions

Fig. 5 shows the filter time dependence of experimental I_{diff} intensities for PIB, Fig. 5 (a), and aPP, Fig. 5 (b), at six different temperatures. In both cases we used $t_f^{min} = 50\mu\text{s}$. There is a remarkable displacement of the curves for longer t_f values as the temperature increases, related to the decrease of the mean correlation time of the motion. Moreover, considering that I_{diff} represents the fraction of segments moving in a dynamic window defined by $t_f^{min} = 50\mu\text{s}$ and t_f , one should expect that I_{diff} reaches 1 only when all segments are moving inside such window. Thus, the increasing in the plateau values of the curves with temperature suggests the distribution of the correlation times getting narrower as the temperature increases. This narrowing is observed for the PIB sample, after performing the Tikhonov regularization to fit the data, as can be seen in Figs. 4 and Fig. 5 (c). To provide an evidence of such behavior we fitted each correlation time distribution of Fig. 5 using log-gaussian functions. The standard deviations of the distributions, as a function of temperature, are shown in Fig. 4, along to the measured values for T_1 . The expected decay of the width of the distribution of correlation times as a function of temperature is observed. There is an almost linear dependence of the standard deviation with the temperature, as assumed in²⁷. However, the width of the distribution of correlation times for the aPP presents an unexpected maximum around 333 K, as seen in Figs. 4 and 5 (d). This distinct behavior of aPP and PIB is explained by comparing the σ vs. T and T_1 vs. T curves, Figs. 4 and 5, in each case. As can be observed, for PIB $T_1 \gg t_f$ in all the measured temperature range, so the effect of T_1 in the magnetization evolution during the dipolar filter can be neglected for all temperatures. However, for temperatures around the minimum of T_1 this is not true for aPP. Indeed, the profiles of σ vs. T and T_1 vs. T are remarkably anti-correlated, suggesting that the apparent broadening of the aPP distribution of correlation times is related to the T_1 relaxation time, when $t_f \approx T_1$. This shows that the estimation of the correlation time distribution by DF-MSE is only reliable if $T_1 \gg t_f^{max}$, where

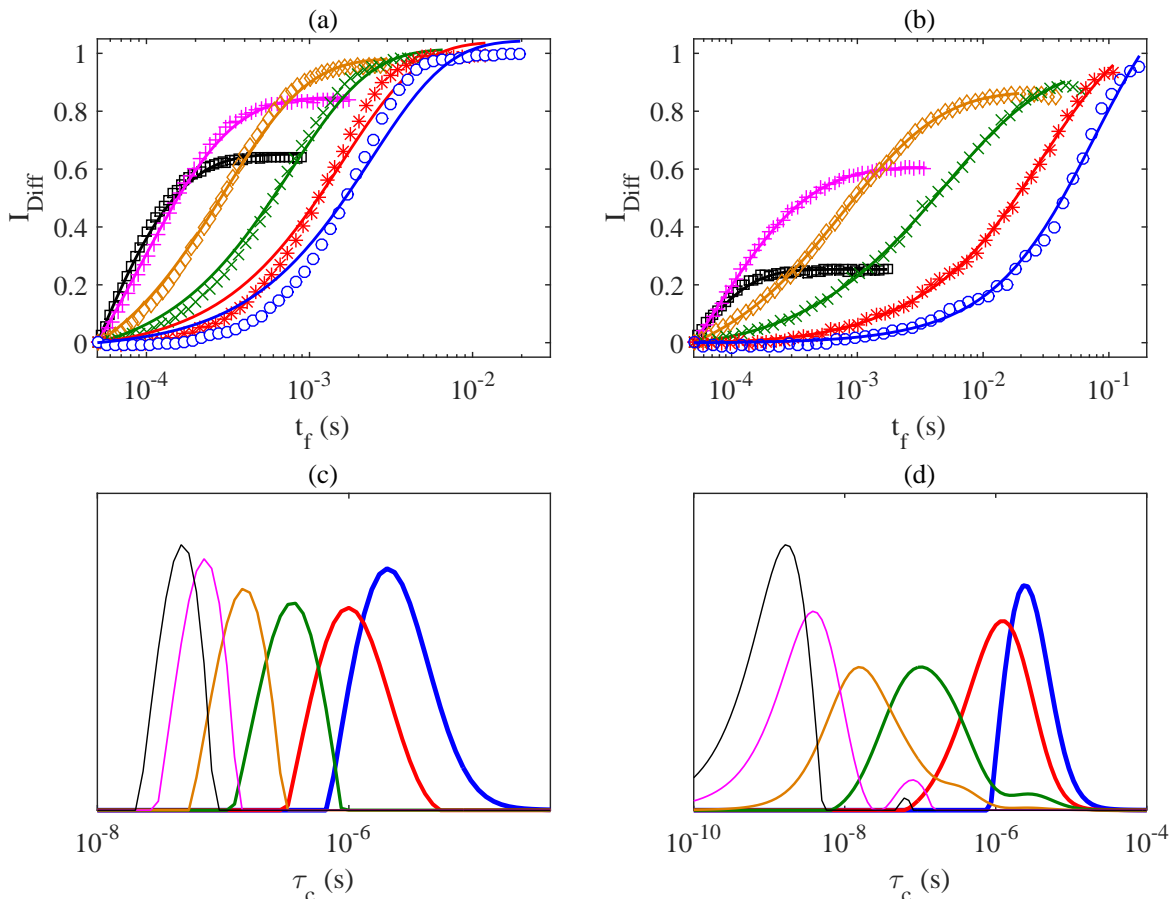


FIG. 5. Fittings and the respective distributions of correlation times for aPP and PIB samples. Above, (a) and (b) show the PIB experimental data and fittings for six different temperatures ($T = 278$ K (black, squares), 293 K (magenta, +), 313 K (orange, diamonds), 333 K (green, \times), 358 K (red, $*$) and 383 K (blue, circles)). Solid lines represent the fittings. The respective distributions obtained are shown in (c) and (d), with the same color scheme as the fittings and data, and line thickness decreasing with the temperature.

t_f^{max} is the longest filter time. All results were obtained without any *a priori* assumption on how the standard deviation behaves with the temperature.

Despite the drawback in the precise estimation of the distribution of correlation times width by DF-MSE, the mean values of this distribution might still be used for providing motion activation parameters. This relies on the observation that $\langle \tau_c \rangle$ dictates the behavior of the I_{Diff} curves for short t_f , when the T_1 effects are still negligible. Furthermore, the mean-values of the distributions obtained from the fittings are used to compare our data with previous experiments, using a Williams-Landelu-Ferry (WLF) activation function,

$$\log_{10} \left(\frac{\langle \tau_c(T) \rangle}{\tau_c(T_g)} \right) = - \frac{C_1(T - T_g)}{C_2 + T - T_g}, \quad (10)$$

where $\langle \tau_c(T) \rangle$ and $\tau_c(T_g)$ are the correlation time at the temperature T and at the glass transition T_g , respectively. C_1 , C_2 and $\tau_c(T_g)$ are fitting parameters.

To support the $\langle \tau_c \rangle$ values obtained for the PIB, we compare our results with a dataset from the literature²⁷. Such data was measured using CODEX experiments, supposing an Arrhenius activation function. We compare the results of such experiments with the ones using the DF-MSE in Fig. 6 (a). The nonlinear behavior typical of the WLF (or VTFH) activation function is clearly observed. The fit by the WLF activation function gives $\tau_c(T_g) = 90 \pm 10$ K, $C_1 = 12.3 \pm 0.1$ and $C_2 = 51 \pm 0.1$ K. Its worth mentioning that the previous measurements were performed using exchange NMR methods, which are sensitive to slower motions, i.e., longer correlation times ($100 \mu\text{s}$ to 1 ms). Thus, they probe τ_c values at lower temperatures, meaning our approach offers an extension of the dynamic window attainable by those previous measurements. The complementarity of the two techniques is remarkable.

To validate the aPP data, we used the same WLF parameters as Zemke *et al*²⁸ and make a comparison

with their ^{13}C NMR relaxation and ^2H NMR exchange data, as shown in Fig. 6 (b). The parameters are $\tau_c(T_g) = 100$ K, $C_1 = 14.5$ and $C_2 = 30$ K. We observe a fair agreement among the different data sets and the WLF function, indicating a consistency between the DF-MSE technique with both ^{13}C relaxometry and $2\text{D } ^2\text{H}$ exchange NMR measurements. Our approach complements the two latter techniques as it is able to detect motions with correlation times in the 10^{-4} to 10^{-6} s range, highlighted by the temperature range between 280 and 300 K of Fig. 6 (b).

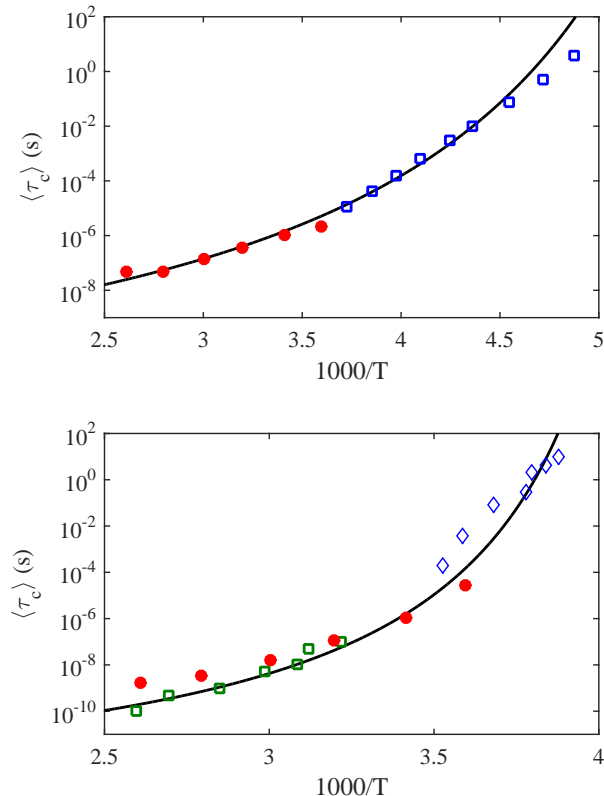


FIG. 6. Mean correlation time for the molecular dynamics of PIB and aPP. Above, the PIB data (red, circles), along with the data from ^{13}C NMR exchange experiments²⁷ (blue, squares). The solid line is the best fit for Eq. 10. The aPP data (red, circles) is shown below, along the results from $2\text{D } ^2\text{H}$ exchange (blue, diamonds) and ^{13}C relaxometry experiments²⁸. The solid line is a plot of the WLF function with $\tau_c(T_g) = 100$ K, $C_1 = 14.5$ and $C_2 = 30$ K, given in²⁸.

IV. DISCUSSION AND CONCLUSIONS

We proposed a simple method to study molecular motions using TD-NMR, based on the Goldman-Shen dipolar filter and in the Anderson-Weiss approximation. The experiment can be used to obtain the onset temperatures

of molecular motions in the kHz-MHz frequency scale, providing an estimation of the temperatures where local or global molecular relations set in. It is also possible to obtain a reliable estimation of the motion parameters, such as, correlation times and their distributions as a function of temperatures, allowing to extract the activation functions of the molecular motions. The estimation of the distribution of correlation times are done using a Tykhonov regularization scheme. A drawback of such procedure is the need of a clean dataset to avoid numerical artefacts in the reconstructed distribution. Moreover, if the signal is long enough to have filter times in the time scale of T_1 , the recovery of magnetization introduces a phase distortion in the signal, resulting in a false broadening of the distribution of correlation times. To avoid big distortions due to T_1 effects, the maximum filter time is limited to T_1 .

Our approach has some advantages when compared to some NMR techniques often employed to probe molecular motions. It is independent on particular choices of activation function^{23,27,47} and the shape of the distribution of correlation times. Furthermore, as the measurements are carried out on the naturally abundant ^1H nuclear spins there is no need to label the samples. This makes the experiments simpler and less expensive, due to the high signal-to-noise ratio. Finally, the DF-MSE sequence allows a very fast acquisition, taking few minutes to obtain one data point and offering a fairly wide dynamic window to probe molecular motions.

V. ACKNOWLEDGEMENTS

The authors gratefully acknowledges financial support from Fundação de Amparo à Pesquisa do Estado de São Paulo (FAPESP), grant numbers [2009/18354-8] and [2008/11675-0], and Conselho Nacional de Desenvolvimento Científico e Tecnológico (CNPq), grant numbers [312852/2014-2], [131489/2014-3], [401454/2014-2] and [300121/2015-6]. E.R.dA thanks Prof. Kay Saalwächter for useful discussions.

REFERENCES

- ¹V. M. Hernandez-Izquierdo, D. S. Reid, T. H. Mchugh, J. D. Berrios, and J. M. Krochta, J. M., J. Food Sci. , 73, 169 (2008).
- ²G. C. Faria, E. R. deAzevedo, H. von Seggern, Macromolecules , 46, 7865 (2013).
- ³G. C. Faria, T. S. Plivelic, R. F. Cossiello, A. A. Souza, T.D.Z. Atvars, I. L. Torriani, E. R. deAzevedo, J. Phys. Chem. B, 113, 11403 (2009).
- ⁴K. Do, Q. Saleem, M. K. Ravva, F. Cruciani, Z. P. Kan, J. Wolf, M. R. Hansen, P. M. Beaujuge, J. L. Bredas, Adv. Mater., 28, 8197 (2016).
- ⁵R. Kurz, A. Achilles, W. Chen, M. Schafer, A. Seidlitz, Y. Golitsyn, J. Kressler, W. G. Paul, G. Hempel,

- T. Miyoshi, T. Thurn-Albrecht, K. Saalwachter, K., *Macromolecules*, 50, 3891 (2017).
- ⁶T. Wang, H. Jo, W. F. H. DeGrado, M. Hong, J. Phys. Chem. B, 119, 4552 (2015).
- ⁷T. J. Simmons, J. C. Mortimer, O. D. Bernardinelli, A. C. Poppler, S. P. Brown, E. R. deAzevedo, R. Dupree, P. Dupree, *Nature Comm.*, 7, 13902 (2016).
- ⁸V. Andronis, G. Zografi, *Pharmaceutical Research*, 15, 835 (1998).
- ⁹E. R. deAzevedo, T. J. Bonagamba and D. Reichert, D., *Prog. Nucl. Magn. Reson. Spect.*, 47, 137 (2005).
- ¹⁰H. W. Spiess, *Macromolecules*, 50, 1761 (2017).
- ¹¹M. H. Hansen, *Chem. Rev.*, 116, 1272 (2016).
- ¹²A. Krushelnitsky, D. Reichert, K. Saalwachter, *Accounts chem. Res.*, 46, 2028 (2013).
- ¹³E. R. deAzevedo, W. G. Hu, T. J. Bonagamba, K. Schmidt-Rohr, *J. Am. Chem. Soc.*, 121, 8411 (1999).
- ¹⁴S. Faske, H. Eckert, M. Vogel, *Phys. Rev. B*, 77, 104301 (2008).
- ¹⁵E. R. deAzevedo, S. B. Kennedy, M. Hong, *Chem. Phys. Lett.*, 321, 43 (2000).
- ¹⁶A. G. Palmer, C. D. Kroenke, J. P. Loria, *Methods Enzym.*, 339, 204 (2001).
- ¹⁷F. Lange, K. Schwenke, M. Kurakazu, Y. Akagi, U. I. Chung, M. Lane, J. U. Sommer, T. Sakai, K. Saalwachter, *Macromolecules*, 44, 9666 (2011).
- ¹⁸W. P. Rothwell, J. S. Waugh, *J. Chem. Phys.*, 74, 2721 (1981).
- ¹⁹M. F. Cobo, K. Malinakova, D. Reichert, K. Saalwachter, E. R. deAzevedo, *Phys. Chem. Chem. Phys.*, 11, 7036 (2009).
- ²⁰K. Schaler, A. Achilles, R. Barenwald, C. Hackel, K. Saalwachter, *Macromolecules*, 46, 7818 (2013).
- ²¹K. Saalwachter, *Macromolecules*, 45, 350 (2012).
- ²²A. Papon, K. Saalwachter, K. Schaler, L. Guy, F. Lequeux, H. Montes, *Macromolecules*, 44, 913 (2011).
- ²³S. Sturniolo and K. Saalwachter, *Chem. Phys. Lett.* 516, 106 (2011).
- ²⁴M. Goldman and L. Shen, *Phys. Rev.* 144, 321 (1966).
- ²⁵S. Matsui, *J. of Magn. Res.* 98, 618 (1992).
- ²⁶P. W. Anderson and P. R. Weiss, *Rev. of Mod. Phys.* 25, 269 (1953).
- ²⁷M. Wachowicz and J. L. White, *Macromolecules* 40, 5433 (2007).
- ²⁸K. Zemke, K. Schmidt-Rohr and H. U. Spiess, *Acta Polymer.*, 45, 148 (1994).
- ²⁹F. Mellinger, M. Wilhelm and H. W. Spiess, *Macromolecules*, 32, 4686 (1999).
- ³⁰D. E. Demco, A. Johansson, and J. T. Tegenfeldt, *Solid State Nucl. Mag. Res.* 4, 13 (1995).
- ³¹K. Schäler, M. Roos, P. Micke, Y. Golitsyn, A. Seidlitz, T. Thurn-Albrecht, H. Schneider, G. Hempel, K. Saalwachter. *Solid State Nucl. Magn. Reson.* 72, 50-63 (2015).
- ³²K. J. Packer and J. M. Pope, *J. of Magn. Res.* 55, 378 (1983).
- ³³A. Wokaun and R. R. Ernst, *Chem. Phys. Lett.* 52, 407 (1977).
- ³⁴E. L. Hahn *Phys. Rev.* 80, 580 (1950); H. Y. Carr, and e. M. Purcell, *Phys. Rev.* 94, 630 (1954); S. Meiboom, and D. Gill, *Rev. Sci. Instrum.*, 29, 688 (1958).
- ³⁵R. H. Boyd, *Polymer* 26, 323 (1985).
- ³⁶R. H. Boyd, *Polymer* 26, 1123 (1985).
- ³⁷R. Bärenwald, Y. Champouret, K. Saalwachter, K. Schäler, *J. Phys. Chem. B* 116, 13089 (2012).
- ³⁸G. Tammann, W. Hesse, *Z. Anorg. Allg. Chem.* 156, 245 (1926). D. Davidson, R. Cole, *J. Chem. Phys.* 19, 1484 (1951). M. L. Williams, R. F. Landel, and J. D. Ferry, *J. Amer. Chem. Soc.* 77, 3701 (1955).
- ³⁹J. H. van Vleck, *Phys. Rev.*, 74, 1168 (1948).
- ⁴⁰J. Hirsinger, *S. S. Nucl. Magn. Reson.*, 34, 210 (2008).
- ⁴¹J. Hirsinger, *Concepts Magn. Reson.*, 28A, 307 (2006).
- ⁴²R. Kimmich. *NMR: tomography, diffusometry, relaxometry*. Berlin: Springer, 1997.
- ⁴³R. Kimmich. *Principles of soft-matter dynamics*. Berlin: Springer, 2012.
- ⁴⁴D. Reichert, K. Saalwachter. *Dipolar coupling: Molecular-level mobility*. eMagRes, 2007.
- ⁴⁵S. Wefing, H. W. Spiess, *J. Chem. Phys.*, 89, 1219 (1988).
- ⁴⁶S. Wefing, S. Kaufmann, H. W. Spiess, *J. Chem. Phys.*, 89, 1234 (1988).
- ⁴⁷M. Wachowicz, L. Gill, J. E. Wolak, J. L. White, *Macromolecules* 41, 2832 (2008).
- ⁴⁸E. R. DeAzevedo, W. G. Hu, T. J. Bonagamba, K. Schmidt-Rohr, *J. of Am. Chem. Soc.* 121, 8411 (1999).
- ⁴⁹E. R. DeAzevedo, T. J. Bonagamba, K. Schmidt-Rohr, *J. Mag. Res.* 142, 86 (2000).
- ⁵⁰E. R. deAzevedo, K. Saalwachter, O. Pascui, A. A. de Souza, T. J. Bonagamba, and D. Reichert. *J. Chem. Phys.* 128, 104505 (2008).
- ⁵¹S. W. Provencher, *Comput. Phys. Commun.* 27, 213 (1982). G. C. Borgia, R. J. S. Brown, and P. Fantazzi, *J. Magn. Res.* 132, 65 (1998).
- ⁵²A. Abragam, *The Principles of Nuclear Magnetism*. Clarendon Press (1961).